Proceedings of the
46th IEEE Conference on Decision and Control
New Orleans, LA, USA, Dec. 12-14, 2007

A Mechanism for Energy Transfer Leading to Conformation Change in Networked Nonlinear Systems

Bryan Eisenhower† and Igor Mezić‡

Abstract— **Understanding mechanisms for conformation change in large networks of biological oscillators leads to comprehension of robustness notions in generic large interconnected dynamical systems. Biological systems are known to be extremely robust to most environmental perturbation while in certain situations they embrace external influence to carry out a particular task. In light of this, the connection with networked or distributed control systems becomes clear. In this paper, we study the dynamical properties of energy transfer through a macromolecule undergoing conformation change. We use a series of dynamical systems tools to identify energy pathways in the system that enable conformation change. We find that during internal resonance, a certain *funneling* structure appears which channels energy in a manner that enables this conformation change to occur.**

I. Introduction

Networks of nonlinear systems often have different pathways for energy transfer and the degree to which their resistance differs often defines the robustness of the system. A system in which all conduits for energy transfer experience the same resistance are relatively robust to a specific perturbation. On the other hand, systems which have one (or a few) paths in which energy transfer is much easier than the average resistance are deemed non-robust because a specific perturbation on this path will dominate its response. In this paper we call these perturbations *structured* as their shape (or direction in phase space) are tuned to the path where the resistance to energy transfer is least (linguistically known as the *sweet spot*, or *weak link*, etc.). These perturbations may result in either desirable or unwanted responses.

In this paper we study a model of a biological macromolecule (DNA-inspired), wherein it is known that the double helix opens and closes as a normal function in certain environmental situations and that the structure of DNA is impervious to most other environmental perturbation. This is a case where a specific perturbation is applied and energy is transferred through the structure of the system effectively to accomplish a particular desired task. As a second example consider the network of nonlinear systems that make up regional power grids. Clearly, it is desired that these systems are impervious to *any* perturbation, while it is found in some situations that specific perturbation effects the system in a major and malicious way (i.e. a tree branch fault resulting in major grid failure).

The mechanism that is essential for energy transfer in networked systems is resonance between the individual units. In linear oscillatory systems, when natural frequencies are near each other, energy transfer is periodic with frequency proportional to the separation in frequencies. In nonlinear systems on the other hand, since frequency and amplitude are dependent, once energy is transferred (and amplitudes change) frequencies are altered and energy may remain in a sink resulting in a nonreversible transfer of energy. This process is termed *energy pumping* or *funneling* and is becoming a popular replacement for linear for passive vibration control (see [1], [2], [3], and [4]). This nonlinear process is facilitated by resonance capture [5] wherein different portions of the phase space have different behavior with respect to energy transfer.

A second mechanism that is often attributed to conformation change in coupled oscillator or molecular systems is that of existence of *discrete* or *multi-breathers*. In this context, spatially localized time periodic solutions initiate global response in the network (see [6]). The excitation of these breathers is commonly known as *Targeted Energy Transfer*. Great progress has been made in this context to understand the conditions needed for this to occur even in biological systems ([7] and [8]). In this paper we are investigating a different response where localized perturbation leads to large (global) coherent motions. In engineering terms, the multi-breather approach seeks traveling wave solutions while we are looking into standing wave behavior.

Below we begin by setting up a case study in terms of its biological background including the discussion of basic dynamical properties of macromolecules (specifically DNA). We then outline the particular model and its derivation. Following this we perform two different canonical transformations to the model in order to illuminate energy transfer mechanisms. We conclude by summarizing the results.

II. Biological Background

The basic construction the DNA helix consists of two linear polymers, each polymer has monomeric units of nucleotides which are connected by Hydrogen bonds. These nucleotides contain sugar, phosphase and a heterocyclic base (can be either A/G: purine, or T/C: pyrimidines). In its physical setting, DNA is typically super-coiled which means that two strands are wound like a helix, connected end to end and then further looped and coiled. Coiling is needed for packing into cells, making the strand more active, or accumulation of energy [9].

The mechanics of DNA evolve on timescales on the order of femtoseconds to seconds. On the nano-second scale (of which we are most interested) we have solid-like motions of

†Student, Department of Mechanical and Environmental Engineering, University of California, Santa Barbara, CA

‡Professor, Department of Mechanical and Environmental Engineering, University of California, Santa Barbara, CA

1-4244-1498-9/07/$25.00 ©2007 IEEE.

sugars, phosphates and bases including: conformation transitions, gene regulation, DNA-protein recognition, and DNA denaturation. This mobility can be caused by many factors including properties of the thermal bath, collisions, influence of local proteins, ion concentration, ph, solvent polarity, or presence of ligands. DNA reacts with drugs, carcinogens, mutants and dyes. As an example of this by stretching and unwinding the double helix, drugs can permeate the DNA structure alternating its properties.

Another important mechanical behavior of DNA is transcription from DNA to RNA. In this process the DNA helix bonds are broken and the chain unzips allowing the RNA polymerase enzyme to bind to one strand of the original DNA helix. This process traverses the length of the strand reading information along the way while opening and closing the Hydrogen Bonds [10].

Mechanically, the separation of the double Helix (unwinding, opening, melting, denaturation, etc.) occurs due to two reasons 1) rotation of the bases, 2) transverse displacements in the strands. Both of these processes result in a relative displacement between the Hydrogen bonds resulting in the separation. In this study we investigate the first mechanism for separation, specifically the separation process and its robustness to external perturbation.

III. The Model

In this section we outline the modeling approach for our particular representation of the DNA strand. There are various ways to model DNA each lending themselves to different physical behavior. A comprehensive review of different modeling approaches can be found in [10]. For our purposes we model coarse grained characteristics including a strong backbone with periodic end conditions and pendula describing the Hydrogen bonds between the two DNA strands. The Hamiltonian is composed of harmonic terms due to torsional coupling between base pairs and anharmonic contributions through a Morse Potential contribution that captures the effect of Hydrogen Bonds between the strand of interest and an its partner strand. To study the dynamical properties of the opening and closing process it is assumed that the partner strand is immobilized.

This model is very similar to the popular Peyrard and Bishop model [11] while their model describes translational motion by way of stretching the Hydrogen bonds and our model considers rotation on the backbone. The model described in this paper is exactly the same as in [12].A schematic of the model can be found in Figure 1 (note that the periodic boundary conditions of the backbone are not in this figure while in the equations of motion).

A. Fundamental Equations of Motion

The nonlinear forces on each pendula are from intermolecular forces between the mobilized and free strand. It is assumed that these nonlinear molecular forces only act from a single free pendula to its immobilized counterpart, cross coupling forces are only included through linear torsional

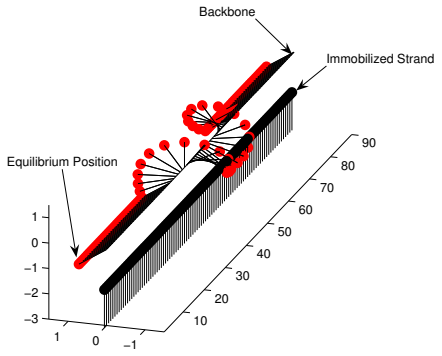

Fig. 1. Schematic representation of the DNA model, two equilibria exist for each pendulum at small angles on either side of the downward position.

contribution along the backbone. The impact of both of these potentials is described below.

The nonlinear force between Hydrogen pairs is not known exactly because its complexity and challenge for experimental verification. Some attempts have been made using AFM and *pull tests* (see [13] for example) and a common potential used for this type of model is the Morse potential. This potential is used because its nonlinear characteristic captures both the attraction from the hydrogen bonds and repulsion from the phosphate groups [14]. The Morse potential is:

$$V_m(y) = D\left(e^{-ay} - 1\right)^2 \tag{1}$$

Where D is the dissociation energy, a is a decay constant, and y is the distance function between interacting molecules.

The distance function used in this model is:

$$y = h\left(1 - \cos\theta_k\right) - x_0 \tag{2}$$

where $k \in (0, N-1)$, N being the number of pendula in the model and θ_k is the angle that the k^{th} pendulum makes with respect to the downward position, x_0 is a equilibrium constant, and h is the length of the pendulum. The coupling of the pendula arises along the backbone through linear torsional effects with the following potential:

$$V_c(\theta_k) = S\frac{1}{2}\left(\theta_{k-1} - \theta_k\right)^2 \tag{3}$$

where S is a constant relating to the torsional stiffness of the backbone. The resulting total potential energy for the system is $V = V_m + V_c$. Considering m as the mass at the tip of the pendulum, from Newtons Laws we have:

$$\begin{aligned} mh^2\ddot{\theta}_k &= -\frac{\partial V(\theta_k)}{\partial\theta_k} = S\left(\theta_{k-1} - 2\theta_k + \theta_{k+1}\right)\ldots \\ &+2ahDe^{a(\cos(\theta_k)h-h+x_0)}\left(e^{a(\cos(\theta_k)h-h+x_0)} - 1\right)\sin(\theta_k) \end{aligned} \tag{4}$$

To simplify the model we rearrange the equation by scaling to absorb $\frac{mh^2}{S}$ into the time variable, and denoting $\frac{2ahD}{S}$ as $\frac{1}{L^2}$. Note that when L is large we have predominately linear dynamics (i.e. $\frac{1}{L^2} \sim \varepsilon$). With this we have the

equations of motion:

$$\begin{array}{l}\dot{\theta}_k = p_k \\ \dot{p}_k = \frac{1}{L^2} e^{a(\cos(\theta_k)h - h + x_0)} \left(-1 + e^{a(\cos(\theta_k)h - h + x_0)}\right) \sin(\theta_k) \\ + (\theta_{k-1} - 2\theta_k + \theta_{k+1})\end{array} \tag{5}$$

where p_k is angular velocity. Using the parameters $\{L = 10, h = 10, a = 0.7, x_0 = 3\}$, for the remainder of this document we reference system of equations (5) as the *nominal model*.

The constant Hamiltonian for this system is:

$$\mathcal{H} = \sum_{k=1}^{N} \frac{p_k^2}{2} + \frac{\left(e^{-a_d(h(1-\cos(\theta_k)) - x_0)} - 1\right)^2}{2a_d h L^2} + \frac{1}{2}\left(\theta_{k-1} - \theta_k\right)^2 \tag{6}$$

At this point, to partially familiarize ourself with the nonlinear aspects of the nominal model we plot contours of constant Hamiltonian in the figure below (Figure 2).

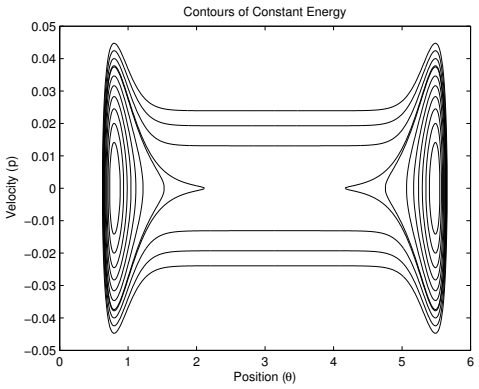

Fig. 2. Energy surface contours for a single pendulum which models a single Hydrogen Bond

The horizontal aspect of the phase space is modular 2π, and we also observe the bistability with two clearly visible potential wells. This bistability is the key feature of the model that facilitates conformation change. That is, we define the two conformations of the system as when all pendula are in one or the other potential well.

Equilibrium analysis of the nominal model illuminates that in fact there exist different equilibria which arise from both the nonlinear and linear potentials. For the nonlinear potential there are four equilibria $\theta_{eq} = \{0, \pi, \pm acos(1 - \frac{x0}{h})\}$ the first two are unstable while the last two are linearly stable. The energy associated with these equilibria are $\{0.03668 \times N, 0.000714 \times N, 0, 0\}$. For the linear potential one equilibrium condition is to have all pendula in a straight line. In summary, the linearly stable equilibria for the entire system is when all pendula are are aligned and at one of the two locations $\pm acos(1 - \frac{x0}{h})$.

It is interesting to note the equilibria condition due to the linear forces, can also be achieved for integer twists of the strand. The dynamics of this system have been investigated to some extent and it has been found that the conclusions from the untwisted model are qualitatively similar to those with a twist, scaled by a constant potential energy. This finding is identical to the conclusion relating to the increase in potential energy barrier for *unzipping* due to the helical twisting as described in [13].

We note here that model derived above is a set of deterministic nonlinear Ordinary Differential Equations. There are various approaches to include the stochastic nature that is unquestionably present in actual molecular setting including temperature themostatting and Langevin arrangements. These aspects have been studied to some extent with this model while we include none of this analysis in this document. The remainder of this paper investigates particular aspects of the nominal model and canonical variants to it. Most of the analysis is performed numerically while driven by analytical insight.

IV. Preliminary Numerical Results

In this section we present numerical simulations and analysis of the nominal model (5) with $N = 30$ molecules. The focus is on the amount of energy vs. the structure of a perturbation to achieve a conformation change. The condition used to determine if the strand has re-conformed, is when the average of the angles exceeds π (straight up in Figure 1). Since this is an unstable equilibrium (saddle), once exceeding this value the strand as a whole is attracted to the second equilibrium.

Because of the scales of concern, conservation of energy is extremely important in simulation of molecular systems. To address the well known problem of numerical dissipation from standard variable step solvers we use geometric integrators which exploit the symplectic structure of the equations of motion. In particular, we use the Verlet method in the Matlab package of Hairer [15].

A. Energy Analysis

In order to determine the sensitivity to structured perturbation, various spatial perturbations were imposed as an initial condition for the position variables, while momenta were set to zero. In particular, perturbation in the structure of spatial Fourier Modes was selected (the reason for this will be made clear later). The amplitude of these perturbations was increased until the DNA strand reconforms and the potential energy of this threshold is recorded. The results of this experiment are presented in Figure 3. An example with a random perturbation is also included for reference.

It is clear from the Figure 3 that with increasing the wavelength of the perturbation more energy is needed to achieve conformation change. We also note that perturbation in a random manner falls within the range of structured perturbation at approximately half of the energy needed for a perturbation of $\frac{N}{2}$ wave number. This makes sense as the random perturbation spreads energy *roughly* equally throughout all wavelengths possible.

V. Modal Projection and Reduction

Due to the spatial invariance (symmetry) and periodic boundary conditions, the empirical eigenfunctions for this

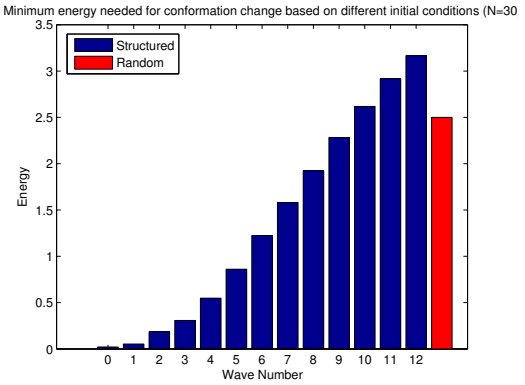

Fig. 3. Energy needed for conformation change as a function of structured perturbation (Fourier Mode)

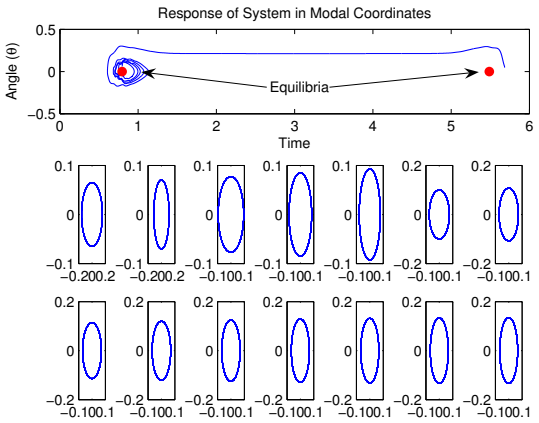

Fig. 4. Response of system in modal coordinates, the first coordinate is highly nonlinear (upper plot, vs. time) while all other coordinates are nearly linear (all other phase space plots).

system are best captured by Fourier Modes. In addition, as we have shown, the energy needed to achieve conformation change is clearly related to the mode shape of the initial perturbation. As such, to get a better understanding of the dynamics, we project the nominal model onto a basis of Fourier Modes using the normalized Discrete Fourier Transform (DFT).

The projection matrix for this procedure and denoted $\mathcal{M}$ and can be found in [16]. This matrix is a $N \times N$ matrix carrying modal information to wavelength $\frac{N}{2}$. As defined, $\mathcal{M}$ is an linear orthogonal matrix which is a symplectic mapping between the original variables and the modal coordinates. The transformed coordinates become (the variables in bold are vectors throughout this document):

$$\left(\hat{\boldsymbol{\theta}}, \hat{\boldsymbol{p}}\right) = \left(\mathcal{M}\boldsymbol{\theta}, \mathcal{M}\boldsymbol{p}\right) \tag{7}$$

With this transformation, we have a decomposed (albeit coupled) system starting with the zeroth mode (the average of all original pendula angles) and modes of increasing spatial wavelength. With an abuse of notation, the general form of the system is:

$$\begin{aligned} \dot{\hat{\boldsymbol{\theta}}} &= \hat{f}\left(\hat{\boldsymbol{\theta}}, \hat{\boldsymbol{p}}\right) \\ \dot{\hat{\boldsymbol{p}}} &= \hat{g}\left(\hat{\boldsymbol{\theta}}, \hat{\boldsymbol{p}}\right) \end{aligned} \tag{8}$$

In Figure 4 we present the the results of a numerical simulation of the system in modal coordinates. The initial conditions are such that all modes greater than zero are perturbed while the zeroth mode remains at equilibrium. The upper-most trace is the response of the zeroth mode vs time, while the phase space of the modes of increasing wavelength are presented from left to right below it. It is evident from this figure that the nonzero modal coordinates experience a nearly linear oscillation. We will find that it is the energy in these modes that eventually is transmitted to the zeroth mode provoking the conformation change.

Because the transformations are canonical, we can remove modes from the system while preserving the Hamiltonian structure. By doing this reduction we will have a more tractable system of equations. We have analyzed the qualitative differences between the full order model and lower order truncations (starting with highest mode first) and have found good agreement (see also [16]). Since the qualitative nature of the model is preserved under reduction, we will use a lower dimensional model for the remainder of the study (the dimension of this reduced model will be denoted M).

VI. Action - Angle Coordinates

To gain further insight into energy transmission characteristics in the model we perform a second canonical transformation to obtain the system in action-angle coordinates. Note that the zeroth mode is already in action-angle coordinates and with this in mind the new system adheres to the following transformation rules:

$$\begin{aligned} \hat{\theta}_0 &\to \phi_0 & \hat{p}_1 &\to J_0 \\ \hat{\theta}_1 &\to \sqrt{\tfrac{2J_1}{\omega_1}}\sin\phi_1 & \hat{p}_1 &\to \sqrt{2J_1\omega_1}\cos\phi_1 \\ &\vdots & &\vdots \\ \hat{\theta}_{\tilde{M}} &\to \sqrt{\tfrac{2J_{\tilde{M}}}{\omega_{\tilde{M}}}}\sin\phi_{\tilde{M}} & \hat{p}_{\tilde{M}} &\to \sqrt{2J_{\tilde{M}}\omega_{\tilde{M}}}\cos\phi_{\tilde{M}} \end{aligned} \tag{9}$$

where $\tilde{M} = M - 1$, $\omega_k = \sqrt{\|\frac{d(\hat{g}_k(\hat{\theta}_k, \hat{p}_k, \epsilon=0))}{d\hat{\theta}_k}\|}$, the k^{th} frequency of the linear system, and M is the number of retained modes. The function $\hat{g}_k$ is obtained from Equation (8). We note at this point that the independent linear natural frequencies (ω_k) for each mode are not rationally commensurate. That is to say, the purely linear portion of the model contains no resonance terms (however, this is not to say that the system never goes into resonance). The resulting form of the system in action-angle coordinates becomes:

$$\begin{aligned} \dot{\phi}_0 &= J_0 & \dot{\phi}_k &= \omega_k + \varepsilon f_k(\boldsymbol{J}, \boldsymbol{\phi}, \varepsilon) \\ \dot{J}_0 &= 0 + \varepsilon g_0(\boldsymbol{J}, \boldsymbol{\phi}, \varepsilon) \quad , & \dot{J}_k &= 0 + \varepsilon g_k(\boldsymbol{J}, \boldsymbol{\phi}, \varepsilon) \end{aligned} \tag{10}$$

where $(J_k,\ \phi_k) \in \mathbb{R} \times \mathbb{R}$ are the k^{th} action and angle for $k = 1, \ldots, M$ and $\omega_k \in \mathbb{R}$ is the rotation number or angular frequency.

Notice that the angle coordinates for all modes with nonzero wavelength have a predominately linear periodic response and the action equations in linear limit are stationary.

A. Numerical Experiments in Action-Angle Coordinates

To illustrate exchange of energy during a targeted initial condition response, we simulate system (10) using a specific initial perturbation. In this case, we simulate a reduced system with seven modes ($M = 7$) with an initial condition on the first mode of $J_1(0) = 0.3$ which is sufficient for conformation change. Figure 5 illustrates the response to this initial perturbation. Only two of the action variables are presented because the others are near zero receiving no energy from the lower order modes throughout the simulation.

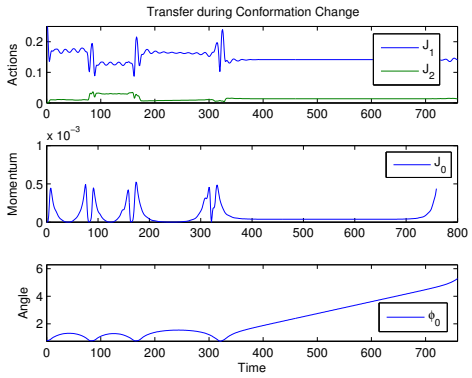

Fig. 5. Time simulations illustrating exchange of action leading up to conformation change

Notice in this figure, that the action behaves stepwise; remaining constant for long periods of time and then at certain times changing abruptly to a different value. This behavior occurs due to internal resonance in the system. That is, at these times the phase space variable of zeroth mode becomes close to one of its equilibria and the system enters a *resonance zone* which enables the energy transfer.

As we have mentioned, internal resonance is a key mechanism for energy transfer in this system. In the Targeted Energy Transfer framework, the system undergoes a *resonance capture* where the variables reach a resonance manifold and remain on this manifold for further time. In our case however, we do not remain in resonance but rather have *passage through resonance* where the system is only in a *resonance zone* for a brief period of time. It is in this time interval that energy transfer occurs.

The resonance conditions for a multi-frequency system are [5]:

$$|(\boldsymbol{\kappa}, \boldsymbol{\omega})| < \frac{1}{c|\boldsymbol{\kappa}|^v} \tag{11}$$

where $(\boldsymbol{\kappa}, \boldsymbol{\omega}) = \kappa_0\omega_0 + \kappa_1\omega_1 + \cdots + \kappa_{M-1}\omega_{M-1}$, κ_i are integers and c, v are positive constants. The quantity on the left hand side of the inequality goes to zero when frequencies become rationally commensurate. The term on the right hand side accounts for resonance in small regions where the frequencies are almost commensurate. In fact the size of the *resonance zone* both in dimension in phase space and time spent inside is related to this value.

To study our system while in resonance, in Figure 6 we plot a few phase variables for the same simulation above (Figure 5). Notice that at instances where the actions undergo their energy transfer (step changes), the difference in frequencies approach zero which is indicative of internal resonance. In fact, in terms of equations (10), the frequencies are constant outside of the resonance zone ($\dot{\phi}_k = \omega_k$) while changing abruptly during resonance the nonlinear element ($f(.)$ of Equations (10)) become active.

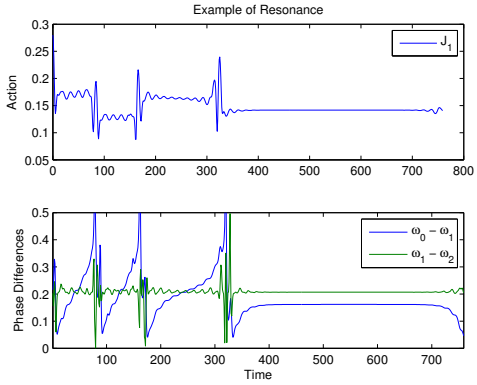

Fig. 6. Relative difference in phase variables as system travels through resonance

B. Analysis of Energy Transfer Mechanisms Resulting in Conformation Change

With the system now in action-angle coordinates (which directly relate to energy) we gain insight into the transmission paths for the modal energy in the system. In particular, we linearize the system and investigate this time dependent operator as the system evolves. What we find is that the structure adheres to a *funneling* behavior wherein energy from higher order modes is transmitted to modes of lower wavelength while transmission in the other direction occurs to a much less extent.

The equation system (10) is linearized analytically without specifying the equilibrium location for this linearization. The form of the resulting system is:

$$\left[\begin{array}{c} \dot{\boldsymbol{\phi}} \\ \dot{\boldsymbol{J}} \end{array}\right] = \left[\begin{array}{c|c} \mathcal{J}_{11} & \mathcal{J}_{12} \\ \hline \mathcal{J}_{21} & \mathcal{J}_{22} \end{array}\right] \left[\begin{array}{c} \boldsymbol{\phi} \\ \boldsymbol{J} \end{array}\right] \tag{12}$$

where each $\mathcal{J}_{ii} \in \mathbb{R}$ is a $M \times M$ matrix.

We are interested in energy transfer and in this system this is represented by change in action. As such, the block $\mathcal{J}_{22}$ becomes important as the change is action is only weakly dependent on angle. Focusing on this lower right submatrix we evaluate it using the data from the numerical experiment

as described in Section VI-A. In Figure 7 we show time averaged values of the $\mathcal{J}_{22}$ block which in this case for a model with seven modes is a 7×7 matrix. The averaging is performed while inside and outside of the resonance zone, and there is a clear distinction between the structure of the system in these two regimes.

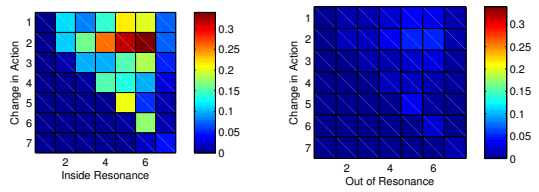

Fig. 7. Time averaged energy transfer operator in and outside of resonance showing a clear preference for energy transfer to lower modes

The interesting behavior of this system occurs in the resonance zones of the phase space where the Jacobian has a clear upper triangular structure while when the system evolves outside, the structure is uniform and of small value. It should be noted at this point that the data presented here is not unique data. Many different numerical experiments were performed with varying parameters (initial conditions etc) with the same qualitative results.

Schematically, this process can be thought of in terms of a directed graph structure for the transfer of energy (see Figure 8). Outside of the resonance zone all paths for energy transfer are uniform. However, in resonance certain directed paths become evident. That is, all high wavelength modes effect the energy in the lower wavelength modes while these same lower order modes do not effect their neighbors of higher wavelength. This explains how a structured perturbation in any mode greater than zero eventually effects the zeroth order mode, and in our case eventually leads to conformation change. This also agrees with the findings in [4] where cascades of irreversible energy transfer occurred due to the preference of modal frequency with the resonant characteristics of the system.

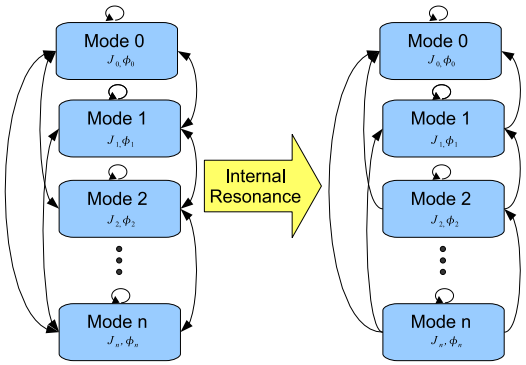

Fig. 8. Schematic of energy transfer pathways during internal resonance

VII. Summary

In this study we have shown that using a series of canonical transformations pathways for energy transfer in a large networked system become evident. Specifically, we find that for a biological macromolecule (DNA), there is a preference for energy transfer through the spatial Fourier Modes from high wavelength towards lower wavelengths. This finding elucidates qualities of robustness to external perturbation for this system. These qualities are particular to the model studied in this paper while they may also describe qualities of other systems including networked control systems.

Acknowledgements

We would like to thank Philip Du Toit and Jerry Marsden for their insight with this problem. In addition, this work was supported under AFOSR grant FA9550-06-1-0088.

References

[1] P. Larsen, P. L. Christiansen, O. Bang, J. Archilla, and Y. B. Gaididei, "Energy funneling in a bent chain of morse oscillators with long-range coupling," *Physical Review E*, vol. 69, no. 2, 2004.
[2] P. N. Panagopoulos, O. Gendelman, and A. F. Vakakis, "Robustness of nonlinear targeted energy transfer in coupled oscillators to changes of initial conditions," *Nonlinear Dynamics*, vol. 47, pp. 377–387, 2007.
[3] G. Kerschen, J. J. Kowtko, D. M. McFarland, L. A. Bergman, and A. F. Vakakis, "Theoretical and experimental study of multimodal targeted energy transfer in a system of coupled oscillators," *Nonlinear Dynamics*, vol. 47, pp. 285–309, 2007.
[4] A. F. Vakakis, D. M. McFarland, L. Berman, L. I. Manevitch, and O. Gendelman, "Isolated resonance captures and resoncance capture cascades leading to single- or multi-mode passive energy pumping in damped coupled oscillators," *Journal of Vibration and Acoustics*, vol. 126, 2004.
[5] V. Arnol'd, ed., *Dynamical Systems III*. Springer-Verlag, 1988.
[6] T. Ahn, R. S. MacKay, and J.-A. Sepulchre, "Dynamics of relative phases: Generalized multibreathers," *Nonlinear Dynamics*, vol. 25, no. 1-3, pp. 157–182, 2001.
[7] A. Memboeuf and S. Aubry, "Targeted energy transfer between a rotor and morse oscillator: A model for selective chemical dissociation," *Physica D*, no. 207, 2005.
[8] S. Aubry, G. Kopidakis, A. Morgante, and G. Tsironis, "Analytic conditions for targeted energy transfer between nonlinear oscillators or discrete breathers," *Physica B*, no. 296, 2001.
[9] A. Vologodskii, *Topology and Physics of Circular DNA*. CRC Press, 1992.
[10] L. Yakushevich, *Nonlinear Physics of DNA*. John Wiley and Sons, 1998.
[11] M. Peyrard and A. R. Bishop, "Statistical mechanics of a nonlinear model for dna denaturation," *Physical Review Letters*, vol. 62, no. 23, 1989.
[12] I. Mezić, "On the dynamics of molecular conformation," *PNAS*, vol. 103, no. 20, pp. 7542–7547, 2006.
[13] S. Cocco, R. Monasson, and M. John, "Force and kinetic barriers to unzipping of the dna double helix," *PNAS*, vol. 98, no. 15, pp. 8608–8613, 2001.
[14] T. Dauxois, M. Peyrard, and A. R. Bishop, "Dynamics and thermodynamics of a nonlinear model for dna denaturation," *Phys. Rev. E*, vol. 47, pp. 684–695, Jan 1993.
[15] E. Hairer, G. Wanner, and C. Lubich, *Geometrical Numeric Integration*. Springer, 2004.
[16] P. D. Toit, J. Marsden, and I. Mezić, "Actuated conformation change in biomolecules," *Physical Review Letters under review*, 2007.